



**HAL**  
open science

## Sound wave velocities of Fe-Ni alloy at high pressure and temperature by mean of inelastic X-ray scattering

Anastasia P. Kantor, Innokenty Yu. Kantor, Alexander V. Kurnosov, Alexei Yu. Kuznetsov, Natalia A. Dubrovinskaia, Michael Krisch, Alexei A. Bossak, Vladimir P. Dmitriev, Vadim S. Urusov, Leonid S. Dubrovinsky

### ► To cite this version:

Anastasia P. Kantor, Innokenty Yu. Kantor, Alexander V. Kurnosov, Alexei Yu. Kuznetsov, Natalia A. Dubrovinskaia, et al.. Sound wave velocities of Fe-Ni alloy at high pressure and temperature by mean of inelastic X-ray scattering. *Physics of the Earth and Planetary Interiors*, 2007, 164 (1-2), pp.83. 10.1016/j.pepi.2007.06.006 . hal-00532119

**HAL Id: hal-00532119**

**<https://hal.science/hal-00532119>**

Submitted on 4 Nov 2010

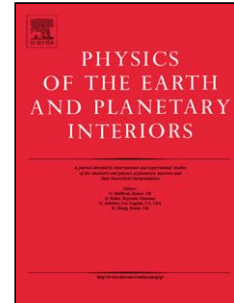
**HAL** is a multi-disciplinary open access archive for the deposit and dissemination of scientific research documents, whether they are published or not. The documents may come from teaching and research institutions in France or abroad, or from public or private research centers.

L'archive ouverte pluridisciplinaire **HAL**, est destinée au dépôt et à la diffusion de documents scientifiques de niveau recherche, publiés ou non, émanant des établissements d'enseignement et de recherche français ou étrangers, des laboratoires publics ou privés.

## Accepted Manuscript

Title: Sound wave velocities of *fcc* Fe-Ni alloy at high pressure and temperature by mean of inelastic X-ray scattering

Authors: Anastasia P. Kantor, Innokenty Yu. Kantor, Alexander V. Kurnosov, Alexei Yu. Kuznetsov, Natalia A. Dubrovinskaia, Michael Krisch, Alexei A. Bossak, Vladimir P. Dmitriev, Vadim S. Urusov, Leonid S. Dubrovinsky



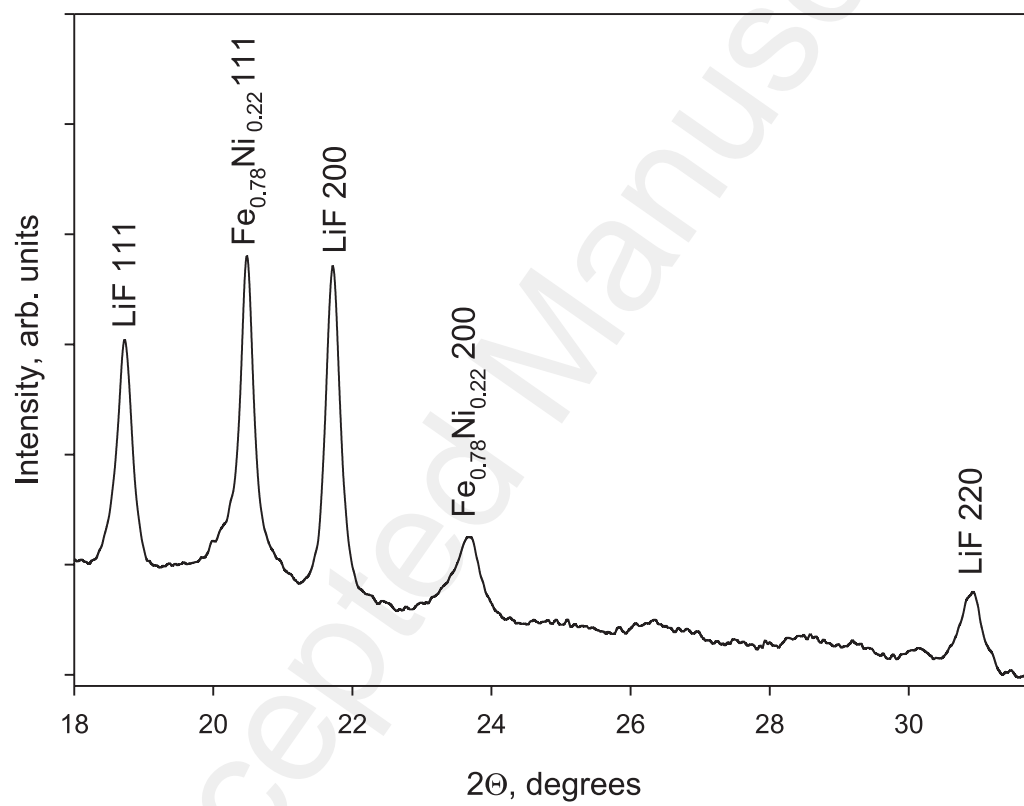
PII: S0031-9201(07)00139-2  
DOI: doi:10.1016/j.pepi.2007.06.006  
Reference: PEPI 4846

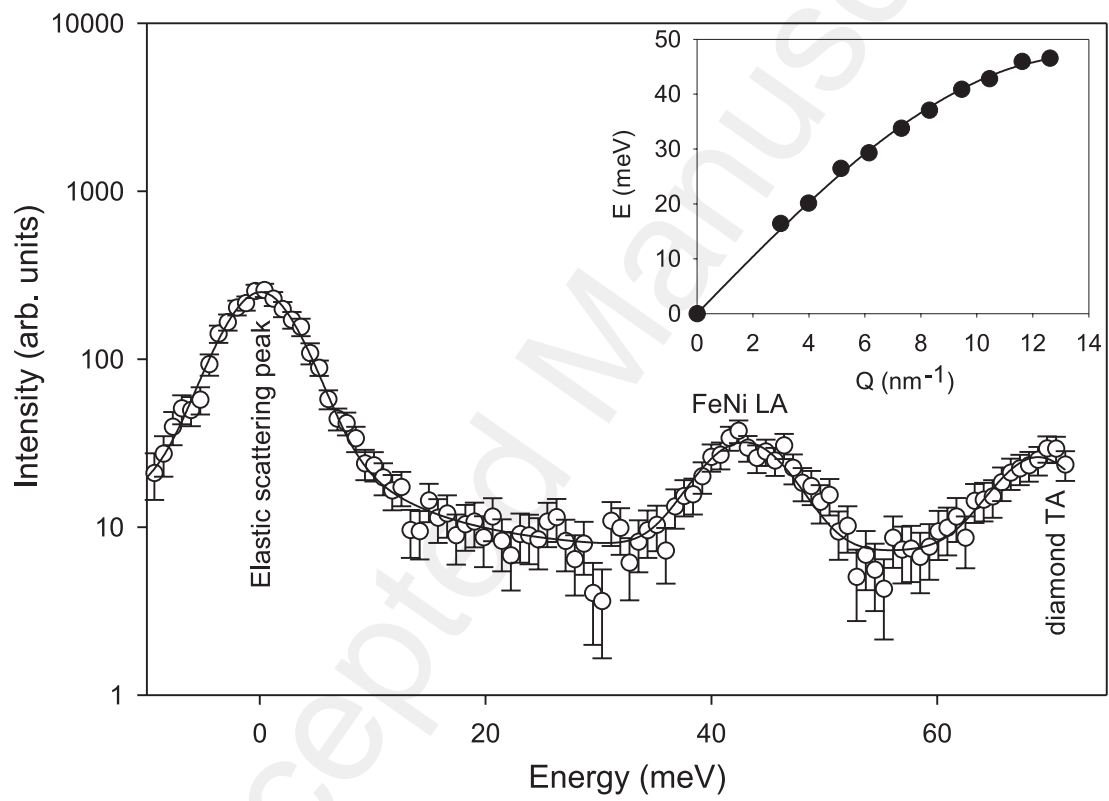
To appear in: *Physics of the Earth and Planetary Interiors*

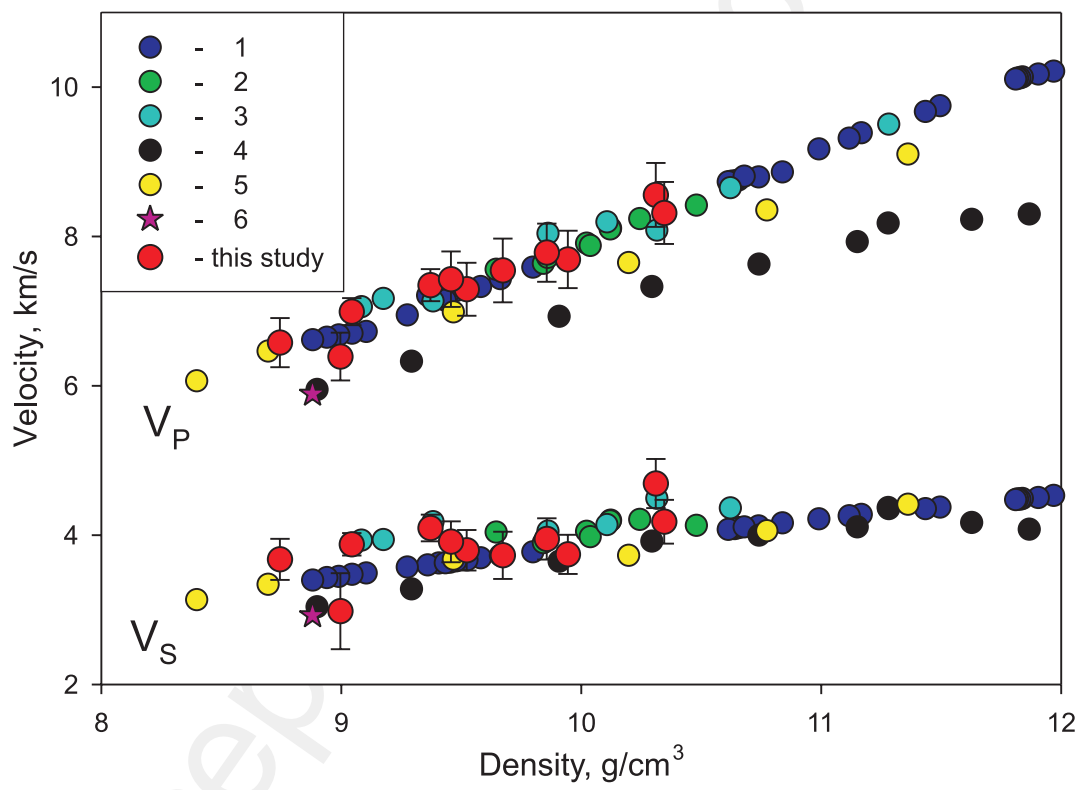
Received date: 19-12-2006  
Revised date: 12-6-2007  
Accepted date: 17-6-2007

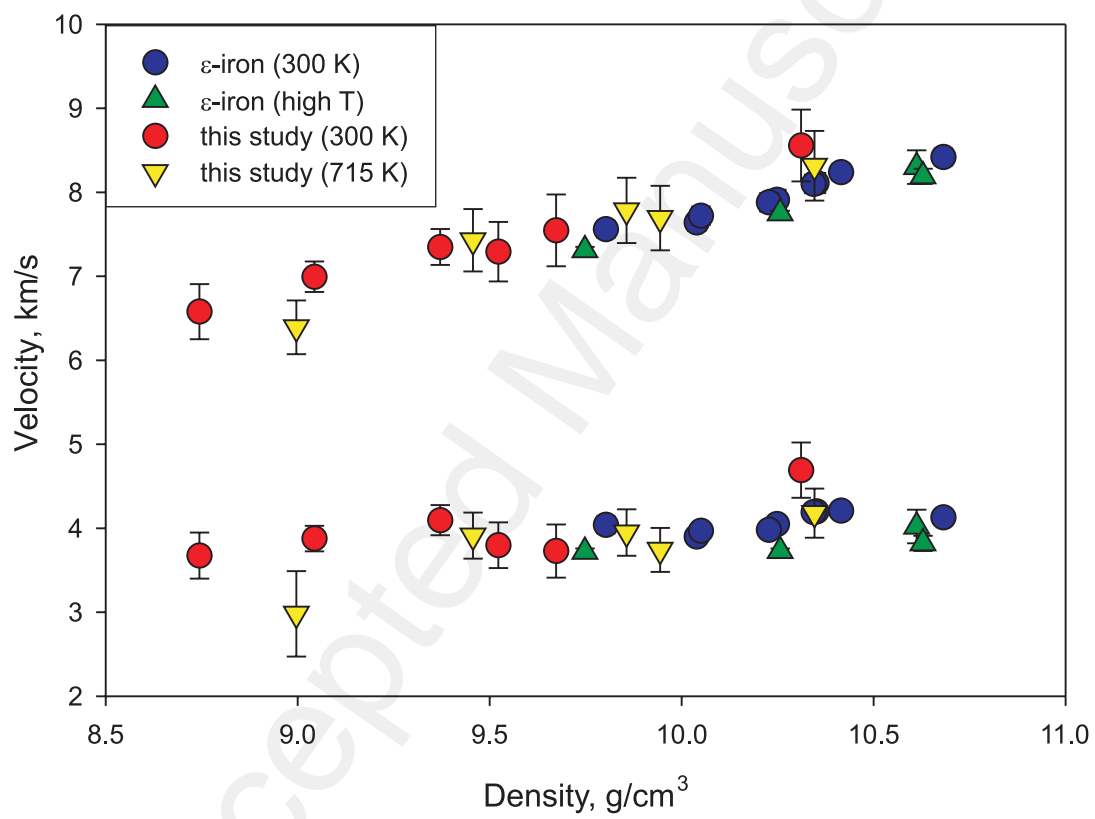
Please cite this article as: Kantor, A.P., Kantor, I.Yu., Kurnosov, A.V., Kuznetsov, A.Yu., Dubrovinskaia, N.A., Krisch, M., Bossak, A.A., Dmitriev, V.P., Urusov, V.S., Dubrovinsky, L.S., Sound wave velocities of *fcc* Fe-Ni alloy at high pressure and temperature by mean of inelastic X-ray scattering., *Physics of the Earth and Planetary Interiors* (2007), doi:10.1016/j.pepi.2007.06.006

This is a PDF file of an unedited manuscript that has been accepted for publication. As a service to our customers we are providing this early version of the manuscript. The manuscript will undergo copyediting, typesetting, and review of the resulting proof before it is published in its final form. Please note that during the production process errors may be discovered which could affect the content, and all legal disclaimers that apply to the journal pertain.









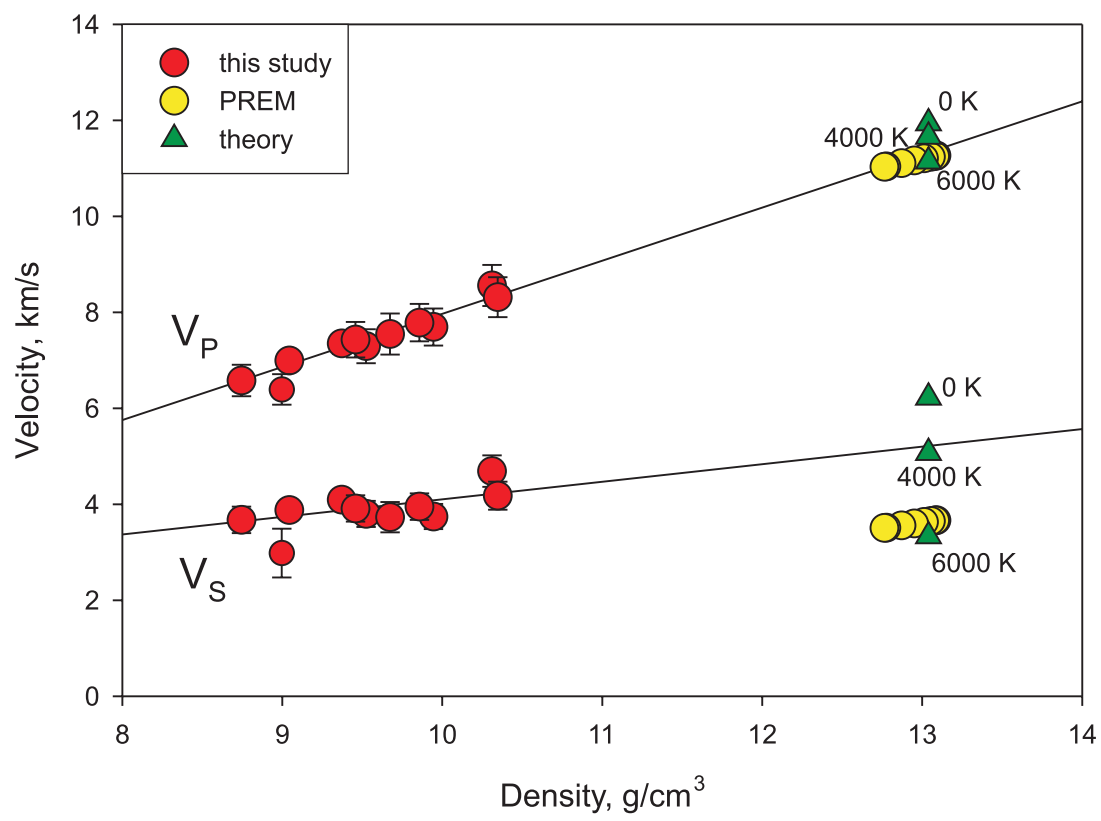


Table 1.

	Pressure, GPa	Density, g/cm <sup>3</sup>	$V_L$ , km/s	$V_T$ , km/s	$K$ , GPa	$G$ , GPa	$\nu$	$E$ , GPa
300 K	12.4 (0.7)	8.74	6.579 (0.3)	3.675 (0.3)	221 (2)	118 (3)	0.2733	301
	20.4 (1.0)	9.04	6.994 (0.2)	3.877 (0.2)	258 (2)	136 (3)	0.2757	347
	30.4 (1.5)	9.37	7.348 (0.2)	4.095 (0.2)	302 (3)	157 (4)	0.2783	402
	35.3 (1.8)	9.52	7.293 (0.4)	3.797 (0.3)	323 (2)	137 (3)	0.3141	361
	40.6 (2.0)	9.67	7.545 (0.4)	3.729 (0.3)	346 (3)	135 (3)	0.3281	357
	65.9 (2.1)	10.31	8.557 (0.4)	4.691 (0.3)	452 (4)	227 (2)	0.2496	583
715 K	21.5 (0.6)	8.997	6.392 (0.3)	2.981 (0.2)	261 (3)	80 (2)	0.2984	218
	37.1 (0.8)	9.457	7.428 (0.4)	3.912 (0.3)	329 (3)	145 (3)	0.2650	379
	52.0 (1.3)	9.857	7.783 (0.4)	3.948 (0.3)	392 (3)	154 (3)	0.2771	408
	54.3 (1.2)	9.945	7.692 (0.4)	3.743 (0.3)	403 (4)	139 (3)	0.2885	375
	71.7 (1.7)	10.35	8.315 (0.4)	4.179 (0.3)	474 (4)	181 (3)	0.2798	481



1 **Sound wave velocities of *fcc* Fe-Ni alloy at high pressure and temperature by mean**  
2 **of inelastic X-ray scattering.**

3

4 Anastasia P. Kantor<sup>1,2,\*</sup>, Innokenty Yu. Kantor<sup>1,2</sup>, Alexander V. Kurnosov<sup>1</sup>, Alexei Yu.  
5 Kuznetsov<sup>1</sup>, Natalia A. Dubrovinskaia<sup>1,3</sup>, Michael Krisch<sup>4</sup>, Alexei A. Bossak<sup>4</sup>, Vladimir  
6 P. Dmitriev<sup>4</sup>, Vadim S. Urusov<sup>2</sup>, Leonid S. Dubrovinsky<sup>1</sup>

7

8 <sup>1</sup> *Bayerisches Geoinstitut, Universitaet Bayreuth, D-95440, Bayreuth, Germany*

9 <sup>2</sup> *Department of Crystallography, Moscow State University, GSP-2, Lenin Hills, Moscow,*  
10 *119992, Russia*

11 <sup>3</sup> *Lehrstuhl fuer Kristallographie, Physikalisches Institut, Universitaet Bayreuth, D-*  
12 *95440 Bayreuth, Germany*

13 <sup>4</sup> *ESRF, 6 rue Jules Horowitz, Grenoble, 38000, France*

14

15 \* Corresponding author. Present address: Bayerisches Geoinstitut

16 Universitaet Bayreuth, D-95440 Bayreuth, Germany. Tel:+49-921-553746; Fax:+49-921-  
17 553769; E-mail: Anastasia.Kantor@Uni-Bayreuth.de

18

19

20 **Abstract**

21 Knowledge of the high-pressure and high-temperature elasticity of Fe-Ni alloy  
22 with low (5-25%) Ni content is crucial for geosciences since it is probably the major  
23 component of the cores of the terrestrial planets and the Moon. Here we present a study

24 of a FeNi alloy with 22 at. % of Ni to 72 GPa and 715 K, using inelastic X-ray scattering  
25 (IXS) and X-ray powder diffraction from polycrystalline material. The X-ray diffraction  
26 (XRD) study revealed stability of the face centred cubic (*fcc*) over the hexagonal close  
27 packed (*hcp*) phase in the whole investigated pressure-temperature range. The study  
28 presents first investigations of elasticity of *fcc* phase of iron-nickel Fe<sub>0.78</sub>Ni<sub>0.22</sub> alloy. The  
29 isothermal equations of state were derived at room temperature and at 715 K  
30 ( $K_{300}=162(1)$  GPa,  $K'_{300}=4.97(1)$ ,  $V_{300}=6.89(1)$  cm<sup>3</sup>/mole;  $K_{715}=160(1)$  GPa,  
31  $K'_{715}=4.97(2)$ ,  $V_{715}=6.96(1)$  cm<sup>3</sup>/mole). Inelastic X-ray inelastic measurements allow the  
32 determination of the longitudinal acoustic wave velocity  $V_p$ , and provide, combined with  
33 the measured equations of state, the full isotropic elasticity of the material. We found that  
34 within experimental errors our data follow the Birch's law. We did not observe any  
35 significant deviations for *fcc* Fe<sub>0.78</sub>Ni<sub>0.22</sub> from elastic properties of pure  $\epsilon$ -iron.

36 Keywords: elasticity, iron-nickel alloy, inelastic scattering, equation of state.

### 37 1. Introduction

38 Properties of major constituents of the Earth's core, iron and its alloys, have long  
39 been of great interest to geophysicists. Cosmochemical data and the composition of iron  
40 meteorites suggest that Earth's core contains a significant (5 to 25 %) amount of nickel  
41 (Anderson, 1989). Iron-nickel alloy with 5-25% Ni content is also thought to be the main  
42 component of the cores of the Mars, Mercury, Moon, satellites of Saturn and Jupiter  
43 (Encrenaz et al., 1995; Robbins et al., 1995; Bottke et al., 2006). Information on the  
44 behaviour of Fe–Ni alloys at high pressure and temperature ( $P$ – $T$ ), such as phase relations  
45 and thermal equations of state (EoS), is essential for interpreting seismic and  
46 geomagnetic observations and for computer modelling of the Earth's deep interior. While

47 pure Fe at high  $P$ - $T$  has been the subject of numerous studies (Mao et al., 1990; Saxena et  
48 al., 1995; Yoo et al., 1995; Boehler, 1993; Andrault et al., 1997; Dubrovinsky et al.,  
49 2000; Crowhurst et al., 2005; Antonangeli et al., 2004), there are far fewer studies on Fe-  
50 Ni alloys (Huang et al., 1988; Lin et al., 2003; Mao et al., 2005; Dubrovinsky and  
51 Dubrovinskaia, 2003).

52 At ambient conditions, the stable phase of  $\alpha$ -Fe has the body-centred cubic (*bcc*)  
53 structure. This phase transforms into a  $\gamma$ -Fe (*fcc*) phase upon increasing temperature  
54 above 1185 K, and then transforms to  $\delta$ -Fe (another *bcc*-structured) phase before melting  
55 (Saxena et al., 1995). At high pressure, both *bcc* and *fcc* phases transform into the  $\epsilon$  (or  
56 *hcp*) phase (Takahashi, Basset, 1964). This phase has a broad stability region, and  $\epsilon$ -Fe is  
57 generally considered to be stable at the inner core conditions (Hemley, Mao, 2001; Ma et  
58 al., 2004). Some theoretical calculations (Belonoshko et al., 2003) predict the *bcc*  
59 structure of iron in this region near the melting temperature, but it was never confirmed  
60 experimentally. Also, the *bcc* phase of Fe could be stabilized at the inner core conditions  
61 by dissolving some amount of “light” elements, in particular, silicon (Vocadlo et al.,  
62 2003; Lin et al., 2002). Pure Ni is thought to be in the *fcc* structure at pressures over 300  
63 GPa and up to the melting temperature (Yoo et al., 2000). The ambient pressure phase  
64 diagram of Fe-Ni alloys shows the existence of both *fcc* and *bcc* phases; the *fcc* phase,  
65 depending on composition, has a complex magnetic behaviour, and is known to exist in  
66 different magnetic states (Hausch and Warlimont, 1973; Dubrovinsky et al., 2001; Meyer,  
67 Entel, 1995). The lower temperature field ( $T < 400$  °C) of the Fe-Ni phase diagram has a  
68 complex configuration that includes a paramagnetic low-Ni disordered *fcc* phase, as well  
69 as the ordered compounds FeNi (tetrataenite) and Ni<sub>3</sub>Fe (Guenzburger and Terra, 2005).

70 The high-pressure phase diagram of Fe-Ni alloys is still not well constrained, and details  
71 of stability fields of *bcc*, *fcc* and *hcp* phases are not clear even for low-Ni (below 25 at%)  
72 alloys (Mao et al., 1990; Huang et al., 1988; Lin et al., 2003; Mao et al., 2005;  
73 Dubrovinsky et al., 2003).

74 Seismological observations provide us constraints concerning pressure, density  
75 and sound wave velocities in the outer liquid and inner solid core, but experimental data  
76 of Fe-Ni elasticity at appropriate conditions are missing. Although sound wave velocities  
77 in pure  $\epsilon$ -iron were measured at high pressures and temperatures (Lin et al., 2005), the  
78 effect of its transition to the  $\gamma$ -phase and on the Ni content were not known so far.  
79 However even relatively small amounts of additional components could change phase  
80 relations and thermophysical properties of iron alloys (Boehler, 1993; Mao et al., 2005;  
81 Lin et al., 2002; Dubrovinsky et al., 2001; Schilfsgaarde et al., 1999; Vidale and Earle,  
82 2000): addition of Ni is thought to increase the *fcc* phase stability field. Therefore, the  
83 understanding and interpretation of composition and properties of the Earth's core (such  
84 as seismic anisotropy, fine-scale heterogeneity, super-rotation (Vidale and Earle, 2000;  
85 Breger et al., 2000)) require detailed studies of the Fe-Ni system at high pressure and  
86 temperature. Here we present the first in situ measurements of the longitudinal sound  
87 velocity  $V_P$  in *fcc*  $\text{Fe}_{0.78}\text{Ni}_{0.22}$  alloy at high pressure and temperature by means of inelastic  
88 X-ray scattering from polycrystalline material. The composition was chosen as one of the  
89 high-end probable Ni-concentrations in the Earth's core in order to see the strongest  
90 possible effect of it on the bulk sound velocities in the alloy. Combined with the  
91 determination of the EoS by X-ray diffraction, we derive as well the transverse velocity  
92  $V_S$ .

## 93           2. Experimental details

94           A single-crystal of iron-nickel alloy containing 22 at% Ni, commercially available  
95 from the IBS company (Germany), was synthesized by the Chochralski method. The  
96 metastable *fcc* crystal, quenched from high temperature, completely transformed to the  
97 polycrystalline *bcc* phase during crystal cutting and polishing, as confirmed by XRD  
98 studies. The sample was polished to a thin plate of about 19  $\mu\text{m}$  thickness, loaded into a  
99 diamond anvil cell and compressed above 12 GPa, so it completely transformed to the  
100 polycrystalline high-pressure *fcc* phase used for further measurements.

101           A four-pin modified Merrill-Basset type DAC (Dubrovinskaia and Dubrovinsky,  
102 2003) equipped with an internal miniature platinum resistive heater was used to compress  
103 and heat the sample. Diamonds with 250  $\mu\text{m}$  culet diameter were used as anvils. A  
104 rhenium gasket with 260  $\mu\text{m}$  initial thickness was preindented to  $\sim 45$   $\mu\text{m}$  and a hole of  
105 125  $\mu\text{m}$  in diameter was drilled. A Fe-Ni sample was loaded along with a large amount  
106 ( $\sim 50$  % of volume) of pure polycrystalline LiF. One of the loadings was performed  
107 without LiF and we didn't observe any difference between experiments with and without  
108 LiF. Several small ruby chips were loaded into the sample chamber for pressure  
109 measurements (Mao et al., 1986). Temperature dependence of the ruby fluorescence was  
110 taken from Rekhi et al., (1999). Temperature was measured using an ultra-thin R-type  
111 thermocouple, located close (within less than 1 mm) to the sample chamber. The  
112 thermocouple was fixed with a ceramic bond on the surface of the metal gasket right near  
113 the diamond/gasket interface.

114           IXS measurements were performed on the ID28 beamline at the European  
115 Synchrotron Radiation Facility in Grenoble, France (Fiquet et al., 2004). The instrument

116 was operated in the Si(888) configuration, with an incident photon energy of 15.817 keV  
117 and a total instrumental energy resolution of 5.5 meV full width at half maximum  
118 (FWHM). The transverse dimensions of the focused X-ray beam of  $25 \times 60 \mu\text{m}^2$   
119 (horizontal  $\times$  vertical, FWHM) were further reduced by slits to approximately  $10 \times 15 \mu\text{m}^2$ .  
120 The momentum transfer  $Q = 2k_i \sin(\theta_s/2)$ , where  $k_i$  is the incident photon wave vector and  
121  $\theta_s$  is the scattering angle, was selected by rotating the spectrometer around a vertical axis  
122 passing through the scattering sample in the horizontal plane. The momentum resolution  
123 was set by slits in front of the analyzers to  $0.25 \text{ nm}^{-1}$ . Energy scans were performed by  
124 varying the monochromator temperature while the analyzer temperature was kept fixed.  
125 Conversion from the temperature scale to the energy scale is accomplished by using the  
126 known thermal expansion coefficient of silicon:  $\alpha(T) = \alpha_0 + \beta(T - T_0)$  with  $\alpha_0 = 2.581 \times 10^{-6}$   
127  $1/\text{K}$  and  $\beta = 0.016 \times 10^{-6} 1/\text{K}^2$ ,  $T_0 = 22.5 \text{ }^\circ\text{C}$  (Bergamin et al., 1997). The validity of this  
128 conversion has been checked by comparing the measured diamond dispersion curve for  
129 longitudinal acoustic phonons with well-established inelastic neutron scattering results.  
130 Two sets of experiments, at room temperature and at 715 (10) K, have been performed.  
131 Before and after each measurement (taking about 10 hours) an in-situ 1-D  
132 monochromatic X-ray diffraction pattern was collected for lattice parameter  
133 determination exactly from the same sample. The final pressure value was calculated  
134 from the lattice parameters (see below).

135 High-pressure and high-temperature angle-dispersive XRD study of the same Fe-  
136 Ni alloy compressed in LiF pressure-transmitting medium was performed using the high-  
137 resolution powder diffractometer of the Swiss-Norwegian BM01 beamline at the ESRF  
138 (Kuznetsov et al., 2002). Sample loading and experimental protocol was exactly the same

139 as for the IXS measurements, in order to avoid any systematic uncertainty. A  
140 monochromatic beam with 0.7995 Å wavelength was used, and the diffracted intensities  
141 were registered with a MAR345 image plate. Experimentally measured pressure-volume  
142 relations at room temperature and at 715 K were reduced to the isothermal third order  
143 Birch-Murnaghan equations of state with a least-square minimization routine. Detailed  
144 results of the XRD study will be given elsewhere.

### 145 **3. Results and discussion**

146 Powder X-ray diffraction reveals that Fe<sub>0.78</sub>Ni<sub>0.22</sub> alloy is stable in the *fcc* phase  
147 throughout the whole studied *P*, *T* range. An example of the analysed integrated pattern  
148 of the spectrum collected at 24.4(2) GPa and room temperature is shown in Fig. 1. The  
149 Debye-Scherrer rings of the studied sample show no evidence of “spotty” diffraction or  
150 inhomogeneous intensity distribution, indicating the absence of notable preferred  
151 orientation. The measured volume in the 20 to 72 GPa pressure range was fitted to the  
152 third order isothermal equations of state at 300 K and at 715 K with the following  
153 coefficients:

$$154 \quad K_{300}=161 (1) \text{ GPa}, K'_{300}=4.97(1), V_{300}=6.89(1) \text{ cm}^3/\text{mole}$$

$$155 \quad K_{715}=160 (1) \text{ GPa}, K'_{715}=4.97(2), V_{715}=6.96(1) \text{ cm}^3/\text{mole}$$

156 All the parameters were fitted, since ambient pressure volume at 300 and 715 K  
157 cannot be measured and is estimated from the obtained EOS. These parameters were used  
158 to calculate the pressure and bulk modulus *K* from the measured volume for every *P-T*  
159 point of the IXS experiment.

160 Fig. 2 shows an example of the IXS spectra collected at the highest reached  
161 pressure (71.7 GPa) and 715 K. It is characterized by an elastic contribution centred

162 around zero energy, and two inelastic features, corresponding to the longitudinal acoustic  
 163 phonons of Fe-Ni and the transverse acoustic phonon of diamond (see Fig. 2). Due to the  
 164 much higher sound velocity ( $\sim 11$  km/s) the diamond contribution moves rapidly out of  
 165 the spectral window of interest with increasing momentum transfer. The energy position  
 166  $E(Q)$  ( $Q$  is the wave vector) of the phonons was extracted using a model function  
 167 composed of several Lorentzians plus Gaussian peak functions, and the number of peak  
 168 components was kept constant for each fit. The origin of small Gaussian smearing of  
 169 inelastic peaks is probably small fluctuations of pressure and temperature during data  
 170 collection, as well as possible pressure gradients and non-systematic instrumental errors.  
 171 This model function was fitted to the IXS spectra, utilizing a standard  $\chi^2$  minimization  
 172 routine. In the case of loading with LiF we also saw its LA phonon, but the contribution  
 173 was clearly apparent due to the higher sound speed in LiF. Transverse phonon modes of  
 174 the  $\text{Fe}_{0.78}\text{Ni}_{0.22}$  alloy cannot be distinguished in our experiment, and only longitudinal  
 175 sound velocities could be obtained directly from IXS measurements. Six to ten  $E(Q)$  (for  
 176  $Q$  from 3 to  $12.6 \text{ nm}^{-1}$ ) values were used to describe the LA phonon dispersions at every  
 177 measured  $P, T$  condition.

178 Within the framework of the Born–von Karman lattice-dynamics theory (Ashcroft  
 179 and Mermin, 1976), the solution of the dynamical matrix can be written as:

$$180 \quad M\omega^2 = \sum_n \Phi_n \left( 1 - \cos \left( \pi \frac{Q}{Q_{\max}} \right) \right), \quad (1)$$

181 where  $M$  is the atomic mass,  $\omega$  is the angular frequency and  $Q$  is the wave vector of the  
 182 considered normal mode,  $Q_{\max}$  is half the distance to the nearest reciprocal lattice point in  
 183 the direction of  $Q$ , and  $\Phi_n$  is the interplanar force constants (the force between an atom



184 and the  $n$ th neighbour plane normal to  $Q$ ). Taking into account only the first term  
 185 (nearest-neighbours interactions) and substituting  $\omega=E/h$  where  $h$  is the Plank constant, it  
 186 can be rewritten as

$$187 \quad E^2 = \frac{h^2 \Phi}{M} \left[ 1 - \cos \left( \pi \frac{Q}{Q_{\max}} \right) \right], \quad (2)$$

188 or, equally

$$189 \quad E = \sqrt{\frac{2h^2 \Phi}{M}} \sin \left( \frac{\pi Q}{2Q_{\max}} \right). \quad (3)$$

190 Taking into account that in long-wavelength limit  $V_P = \frac{2\pi}{h} \frac{\partial E}{\partial Q}$  with  $Q$  equals to zero, the  
 191 final result is

$$192 \quad E = \frac{h}{\pi^2} Q_{\max} V_P \sin \left( \frac{\pi Q}{2Q_{\max}} \right), \quad (4)$$

193 or, equally

$$194 \quad V_P = \frac{\pi^2}{h} E \left[ Q_{\max} \sin \left( \frac{\pi Q}{2Q_{\max}} \right) \right]^{-1}, \quad (5)$$

195

196 where  $V_P$  is the longitudinal (compressional) sound wave velocity. Values for  $V_P$  were  
 197 consequently derived from the equation 5, with  $Q_{\max}$  left as a free parameter (Fig.2,  
 198 inset). Although intrinsic anisotropy of the material could still produce some anisotropy  
 199 even in an orientationally averaged polycrystalline sample, this effect is probably  
 200 negligible, and we consider our sample as an isotropic polycrystalline material. In this  
 201 case, the measured  $V_P$  is the bulk longitudinal sound velocity, and the transverse (shear)  
 202 sound velocity  $V_S$  was obtained according to the relation:

$$203 \quad V_S^2 = \frac{3}{4} \left( V_P^2 - \frac{K}{\rho} \right), \quad (6)$$

204 where  $\rho$  is the density and  $K$  is the adiabatic bulk modulus. In this equation the isothermal  
205 (instead of adiabatic) bulk modulus was used. Numerical estimates show that the  
206 difference between  $K_T$  and  $K_S$  in our case is negligible (less than 2 %). Values of the  
207 isothermal bulk modulus  $K$  for a given density  $\rho$  were calculated from measured EoS  
208 parameters (see above). The values of other generally used isotropic elastic moduli (shear  
209 modulus  $G$ , Young's modulus  $E$ , and Poisson's ratio  $\nu$ ) could be easily calculated and are  
210 listed in table 1 along with  $V_P$  and  $V_S$  values.

211 Sound wave velocities, plotted against density, are shown in Fig. 3. Our data for  
212 *fcc* Fe<sub>0.78</sub>Ni<sub>0.22</sub> are in good agreement with those for  $\epsilon$ -iron and iron-nickel alloy  
213 measured by Lin et al. (2003) (Fig. 3A). The sound velocities for pure *hcp*-Co and Ni are  
214 systematically lower at the same density. This difference cannot be explained by the  
215 atomic mass difference only, implying that simple mass corrections to the alloys elastic  
216 properties are invalid.

217 The well-known linear relation between longitudinal velocities and density (so  
218 called "Birch's law") (Birch, 1961) that is usually used in geosciences for extrapolations  
219 to the Earth's inner core conditions is generally satisfied within the uncertainties of our  
220 measurements. Our IXS study shows no detectable difference between room and high  
221 temperature results when normalized to density (Fig. 3B). The only exception is one  
222 high-temperature point at pressure 21.5 GPa, which is notably lower. This point could  
223 accidentally fall into narrow pressure and temperature region with anomalous  
224 compressibility in FeNi alloy also known as the invar effect (Dubrovinsky et al., 2001)

225 and thus the elastic behaviour of *fcc* Fe<sub>0.78</sub>Ni<sub>0.22</sub> alloy at low pressure (<25 GPa) region  
226 require additional studies. The absence of a significant temperature effect on  $V_P$  agrees  
227 with theoretical calculations (Steinle-Neumann et al., 2001): even at temperatures about  
228 4000 K, longitudinal sound wave velocities in  $\epsilon$ -iron are thought to decrease only by 2-  
229 3% (Fig. 3C). We can suppose that at  $T < 1000$  K the temperature effect is not detectable  
230 with the present experimental accuracy. In contrast to this, a recent nuclear-resonant  
231 inelastic x-ray scattering study (Lin et al., 2005) reported that  $\epsilon$ -iron does not follow  
232 Birch's law at high temperatures, and that sound velocities significantly decrease with  
233 temperature for a given density. Our results could not confirm such anomaly for Fe-Ni  
234 alloy in studied pressure – temperature range.

235         When extrapolate our data to Earth's inner core conditions and compare with  
236 PREM (Dziewonski and Anderson, 1981), almost no difference can be seen in  
237 longitudinal wave velocities, but  $V_S$  is significantly higher than the values expected in  
238 Earth's core (Fig. 3C). If we assume similar temperature corrections as for pure  $\epsilon$ -iron  
239 (Steinle-Neumann et al., 2001), both  $V_P$  and  $V_S$  would be below the PREM model for *fcc*  
240 Fe<sub>0.78</sub>Ni<sub>0.22</sub> alloy. Could this difference be attributed to the presence of "light" elements,  
241 such as oxygen or sulphur, in the inner core? It is known that the density of the core is  
242 somewhat lower than what is expected for pure iron or iron-nickel alloy at corresponding  
243 conditions (Dziewonski and Anderson, 1981; Dubrovinsky et al., 2001). Incorporation of  
244 a few percent of "light" elements to the core could solve the problem. At the same time  
245 "light" elements would influence elastic properties of the core, and also increase sound  
246 velocities. For example, numeric estimations for addition of silicon in form of FeSi-alloy

247 to pure iron would result in decreasing density and increasing sound wave velocities (Lin  
248 et al., 2003).

249 Previous studies (Mao et al., 2005; Huang et al., 1992) in combination with the  
250 present work show that there is still no unambiguous answer about phase stability fields  
251 of *bcc*, *fcc* and *hcp* structures of FeNi alloys with different content of Ni under high  
252 pressure. It is clear that even small changes in Ni content result in dramatic changes of  
253 the *fcc* stability field. In our case (22 at. % of Ni) the stability field of the *fcc* phase is  
254 larger than was reported by Mao et al. (2005) for  $\text{Fe}_{0.95}\text{Ni}_{0.05}$ ,  $\text{Fe}_{0.85}\text{Ni}_{0.15}$ ,  $\text{Fe}_{0.80}\text{Ni}_{0.20}$  and  
255 by Huang et al. (1992) for  $\text{Fe}_{0.70}\text{Ni}_{0.30}$ .

#### 256 4. Conclusions

257 High-pressure and high-temperature (up to 72 GPa and 715 K) study of *fcc*  
258  $\text{Fe}_{0.78}\text{Ni}_{0.22}$  alloy was performed. The X-ray diffraction study revealed stability of the *fcc*  
259 over *hcp* phase in the whole studied  $P$ ,  $T$  range. An isothermal equation of state was  
260 derived at room temperature and at 715 K. X-ray inelastic scattering measurements  
261 allowed the longitudinal acoustic wave velocity to be measured that gives, combined with  
262 measured EoS, the full isotropic elasticity of the material. We did not observe a  
263 significant deviation of the elastic properties from those of pure  $\epsilon$ -iron and furthermore  
264 no deviation from Birch's law. Although the bulk elasticity of *fcc* Fe-Ni alloy and  $\epsilon$ -Fe  
265 seem to be very similar, the elastic anisotropy (directions of the fast and slow waves) of  
266 the hexagonal  $\epsilon$ -Fe and cubic Fe-Ni should be quite different (Cohen et al., 1997). If the  
267 metal phase in the inner core is not hexagonal, but cubic (or a mixture of the two phases  
268 exists) anisotropy may provide a better way to discriminate between the two.

269            **Acknowledgments**

270            This study was supported by ESF, DFG and Russian Federation Government  
271 support of the leading scientific schools. We highly appreciate the discussions with C.  
272 McCammon and Y. Volkova.

Accepted Manuscript

273

**References**

- 274 Anderson, D., 1989. Theory of Earth. Blackwell Scientific Publications, Oxford, 366 pp.
- 275 Andraut, D., Fiquet, G., Kunz, M., Visocekas, F., and Häusermann, D., 1997. The  
276 orthorhombic structure of iron: an *in situ* study at high-temperature and high-pressure.  
277 Science, 278: 831-834.
- 278 Antonangeli, D., Krisch, M., Fiquet, G., Badro, J., Farber, D.L., Bossak, A., and Merkel,  
279 S., 2005. Aggregate and single-crystalline elasticity of hcp cobalt at high pressure. Phys.  
280 Rev. B, 72: 1343031-1343037.
- 281 Antonangeli, D., Occelli, F., Requardt, H., Badro, J., Fiquet, G., and Krisch, M., 2004.  
282 Elastic anisotropy in textured hcp-iron to 112 GPa from sound wave propagation  
283 measurements. Earth and Planet. Sci. Lett., 225: 243-251.
- 284 Ashcroft, N.W., and Mermin, N.D., 1976. Solid state physics. Saunders College  
285 Publishing & Harcourt Brace College Publishers, Orlando, 826 pp.
- 286 Belonoshko, A.B., Ahuja, R., and Johansson, B., 2003. Stability of the body-centred-  
287 cubic phase of iron in the Earth's inner core. Nature, 424: 1032-1034.
- 288 Bergamin, A., Cavagnero, G., Mana, G., and Zosi, G., 1997. Lattice parameter and  
289 thermal expansion of monocrystalline silicon. J. Appl. Phys., 82: 5396-5400.
- 290 Birch, F., 1961. Composition of the Earth's Mantle. Geophys. J. R. Astron. Soc., 4: 295-  
291 311.
- 292 Boehler, R., 1993. Temperatures in the Earth's core from melting-point measurements of  
293 iron at high static pressures. Nature, 363: 534-536.

- 294 Bottke, W.F., Nesvorny, D., Grimm, R.E., Morbidelli, A., and O'Brien, D.P., 2006. Iron  
295 meteorites as remnant of planetesimals formed in the terrestrial planet region. *Nature*,  
296 439: 821-824.
- 297 Breger, L., Romanowicz, B., and Rousset, S., 2000. New constraints on the structure of  
298 the inner core from P'P'. *Geophys. Res. Lett.*, 27: 2781-2784.
- 299 Cohen, R.E., Stixrude, L., and Wasserman, E., 1997. Tight-binding computations of  
300 elastic anisotropy of Fe, Xe, and Si under compression. *Phys. Rev. B*, 56: 8575-8589.
- 301 Crowhurst, J.C., Goncharov, A.F., and Zaug, J.M., 2005. Direct measurements of the  
302 elastic properties of iron and cobalt to 120 GPa – implications for the composition of  
303 Earth's core. In: J. Chen, Y. Wang, T.S. Duffy, G. Shen, L.F. Dobrzhinetskaya (Editors).  
304 *Advanced in high-pressure technology for geophysical applications*. Elsevier,  
305 Amsterdam: 3-23.
- 306 Dubrovinskaia, N.A., and Dubrovinsky, L.S., 2003. Whole-cell heater for the diamond  
307 anvil cell. *Rev. Sci. Instrum.*, 74: 3433-3437.
- 308 Dubrovinsky, L.S., and Dubrovinskaia, N.A., 2003. High pressure crystallography at  
309 elevated temperatures: experimental approach. In: Katrusiak, A., and McMillan, P.  
310 (Editors). *High-pressure crystallography. Mathematics, Physics and Chemistry*, 40.  
311 Kluwer Academic Publishers: 393-410.
- 312 Dubrovinsky, L.S., Dubrovinskaia, N.A., Abrikosov, I.A., Vennström, M., Westman, F.,  
313 Carlson, S., Schilfgaard, M. Van, and Johansson, B., 2001. Pressure induced Invar effect  
314 in Fe-Ni alloys. *Phys. Rev. Letters*, 86: 4851-4854.

- 315 Dubrovinsky, L.S., Dubrovinskaia, N.A., and Le Bihan, T., 2001. Aggregate sound  
316 velocities and acoustic Grueneisen parameter of iron up to 300 GPa and 1200 K. PNAS,  
317 98: 9484-9489.
- 318 Dubrovinsky, L.S., Saxena, S.K., Tutti, F., and Le Bihan, T., 2000. X-ray study of  
319 thermal expansion and phase transition of iron at multimegabar pressure. Phys. Rev.  
320 Letters, 84: 1720-1723.
- 321 Dziewonski, A.M., and Anderson, D.L., 1981. Preliminary reference Earth model. Phys.  
322 Earth Planet. Inter., 25: 297–356.
- 323 Encrenaz, T., Bibring, J.-P., and Blanc, M., 1995. The Solar System. Springer-Verlag  
324 Berlin Heidelberg, 350 pp.
- 325 Fiquet, G., Badro, J., Guyot, F., Bellin, Ch., Krisch, M., Antonangeli, D., Requardt, H.,  
326 Mermet, A., Farber, D., Aracne-Ruddle, C., and Zhang, J., 2004. Application of inelastic  
327 X-ray scattering to the measurements of acoustic wave velocities in geophysical materials  
328 at very high pressure. Phys. Earth Planet. Int., 143/144: 5–18.
- 329 Guenzburger, D., and Terra, J., 2005. Theoretical study of magnetism and Mössbauer  
330 hyperfine interactions in ordered FeNi and disordered fcc Fe-rich Fe–Ni alloys. Phys.  
331 Rev. B, 72: 0244081-0244089.
- 332 Hausch, G., and Warlimont, H., 1973. Single crystalline elastic constants of  
333 ferromagnetic face centred cubic Fe-Ni invar alloys, Acta Metallurgica, 21: 401-414.
- 334 Hemley, R.J., and Mao, H.K., 2001. In-situ studies of iron under pressure: New windows  
335 on the Earth's core. Intern. Geol. Rev., 43: 1–30.
- 336 Huang, E., Basset, W., and Weathers, M.S., 1988. Phase relations in Fe-Ni alloys at high  
337 pressures and temperatures. J. Geophys. Res., 93: 7741-7746.



- 338 Huang, E., Basset, W., and Weathers, M.S., 1992. Phase diagram and elastic properties of  
339 Fe 30 % Ni alloy by synchrotron radiation. *J. Geophys. Res.*, 97: 4497-4502.
- 340 Kuznetsov, A., Dmitriev, V., Dubrovinsky, L., Prakapenka, V., and Weber, H.P., 2002.  
341 FCC-HCP phase boundary in lead. *Solid State Commun.*, 122: 125-127.
- 342 Lin, J.-F., Heinz, D. L., Campbell, A.J., Devine, J.M., and Shen G., 2002. Iron-silicon  
343 alloy in Earth's core? *Science*, 295: 313-315.
- 344 Lin, J.-F., Struzhkin, V.V., Sturhahn, W., Huang, E., Zhao, J., Hu, M.Y., Alp, E.E.,  
345 Mao, H.K., Boctor, N., and Hemly R.J., 2003. Sound velocities of iron-nickel and iron-  
346 silicon alloys at high pressures. *Geophys. Res. Lett.*, 30: 21121-21124.
- 347 Lin, J.-F., Sturhahn, W., Zhao, J., Shen, G, Mao, H.K., and Hemly R.J., 2005. Sound  
348 velocities of hot dense iron: Birch's law revised. *Science*, 308: 1892-1894.
- 349 Ma, Y., Somayazulu, M., Shen, G, Mao, H.K., Shu, G., and Hemley R.H., 2004. In situ  
350 X-ray diffraction studies of iron to Earth-core conditions. *Phys. Earth Planet. Int.*,  
351 143/144: 455– 467.
- 352 Mao, H.K., Wu, Y., Chen, L.C., Shu, J.F., and Jephcoat, A.P., 1990. Static compression  
353 of iron to 300 GPa and Fe<sub>0.8</sub>Ni<sub>0.2</sub> alloy to 260 GPa: implications for composition of the  
354 core, *J. Geophys. Res.*, 95: 21737-21742.
- 355 Mao, H.K, Xu, J., and Bell, P.M, 1986. Calibration of the ruby pressure gauge to 800  
356 kbar under quasi-hydrostatic conditions. *J. Geophys. Res.*, 91: 4673-4678.
- 357 Mao, W.L., Campbell, A.J., Heinz, D.L., and Shen, G., 2005. Phase relations of Fe-Ni  
358 alloys at high pressure and temperature. *Phys. Earth Planet. Int.*, 155: 146-151.
- 359 Meyer, R., and Entel P., 1995. Molecular dynamics study of iron-nickel alloys. *Journal*  
360 *de Physique IV*, 5: 123-128.

- 361 Rekhi, S., Dubrovinsky, L.S., and Saxena, S.K., 1999. Temperature-induced ruby  
362 fluorescence shifts up to a pressure of 15 GPa in an externally heated diamond anvil cell  
363 High Pres.-High Temp., 31: 299-305.
- 364 Robbins, R.R., Jefferys, W.H., and Shawl, S.J., 1995. Discovering astronomy. John  
365 Wiley and sons, Inc., 540 pp.
- 366 Saxena, S.K., Dubrovinsky, L.S., Haggkvist, P., Cerenius, Y., Shen, G., and Mao, H.K.,  
367 1995. Synchrotron x-ray study of iron at high pressure and temperature. Science, 269:  
368 1703-1704.
- 369 Schilfgaarde, M., Abrikosov, I.A., and Johansson, B., 1999. Origin of the Invar effect in  
370 iron-nickel alloys. Nature, 400: 46-49.
- 371 Steinle-Neumann, G., Stixrude, L., Cohen, R.E., and Gülseren, O., 2001. Elasticity of  
372 iron at the temperature of the Earth's inner core. Nature, 413: 57-60.
- 373 Takahashi, T., and Bassett, W.A., 1964. A high pressure polymorph of iron. Science, 145:  
374 483-486.
- 375 Vidale, J.E., and Earle, P.S., 2000. Fine-scale heterogeneity in the Earth's inner core.  
376 Nature, 404: 273-275.
- 377 Vocadlo, L., Alfe, D., Gillan, M.J., Wood, I.J., Brodholt, J.P., and Price, G.D., 2003.  
378 Possible thermal and chemical stabilization of body-centred-cubic iron in the Earth's  
379 core. Nature, 424: 536-539.
- 380 Yoo, C.S., Akella, J., Campbell, A.J., Mao, H.K., and Hemley, R.J., 1995. Phase diagram  
381 of iron by in situ x-ray diffraction: implications for Earth's core. Science, 270: 1473-  
382 1475.

- 383 Yoo, C.S., Cynn, H., Söderlind, P., and Iota, V., 2000. New  $\beta$ (fcc)-cobalt to 210 GPa.  
384 Phys. Rev. Lett., 84: 4132-4135.

Accepted Manuscript

**Figure and table captions.**

Fig.1. Typical example of analysed integrated XRD patterns of the spectrum collected at 24.4 GPa and room temperature.

Fig. 2. Representative IXS spectrum of polycrystalline  $\text{Fe}_{0.78}\text{Ni}_{0.22}$  alloy, collected at 71.7 GPa and 715 K ( $Q=10.45 \text{ nm}^{-1}$ ). Inset: an example of the sinusoidal fit to the experimental  $E(Q)$  relation.

Fig. 3. Sound velocities of  $\text{Fe}_{0.78}\text{Ni}_{0.22}$  alloy at ambient and high temperature (red circles) in comparison with: A - data for pure  $\epsilon$ -iron: 1 – Dubrovinsky et al. (2001), 2 – Lin et al. (2005), 3- Antonangeli et al. (2004), *hcp* Co – 4 (Antonangeli et al., 2005),  $\text{Fe}_{0.87}\text{Ni}_{0.13}$  alloy – 5 (Lin et al., 2003) and 6 - sound wave velocities for pure *fcc* Ni at ambient conditions; B –high and room temperature data for  $\epsilon$ -iron (Lin et al., 2005) and *fcc*  $\text{Fe}_{0.78}\text{Ni}_{0.22}$  alloy (this study); C - our data (line shows linear fit to our data extended to the inner core conditions) in comparison with the seismic observations (PREM) (Dziewonski and Anderson, 1981) and calculated sound wave velocities for  $\epsilon$ -iron at different temperatures (Steinle-Neumann et al., 2001).

Table 1. Aggregate longitudinal and transverse velocities, bulk, shear, Young's moduli and Poisson ratio of *fcc*  $\text{Fe}_{0.78}\text{Ni}_{0.22}$  alloy as obtained from IXS and X-ray diffraction measurements.